A New Experimentally Validated Archetype for Model Predictive Control of Residential Buildings with Heat Pump

Alice Mugnini[1*], *Maarten* Evens[2,3], *Fabio* Polonara[4] and *Alessia* Arteconi[2,3]

[1]Department of Theoretical and Applied Sciences, Università E-Campus, Novedrate 22060, Italy
[2]Department of Mechanical Engineering, KU Leuven, 3001 Leuven, Belgium
[3]EnergyVille, 3600 Genk, Belgium
[4]Department of Industrial Engineering and Mathematical Sciences (DIISM), Università Politecnica delle Marche, Ancona, 60131, Italy

Abstract. Model Predictive Control (MPC) provides efficient control of building heating systems, integrating comfort and energy goals. However, widespread implementation remains constrained by the computational complexity of predictive models and the challenges of controlling advanced thermal distribution systems, particularly those with heat pumps. To address these limitations, the authors previously proposed several MPC archetypes that simplify design and enable large-scale use. Experimentally validated on a real heat pump system, they cover three heating setups, namely low-temperature radiators without storage, with integrated storage, and underfloor heating. The present study extends this framework by introducing a novel archetype specifically developed for heat pump systems with underfloor heating and an external thermal energy storage. The MPC minimizes an objective function configurable via a user-selected penalty signal, such as electricity price, primary energy consumption, or other operational criteria. This work presents the archetype and demonstrates its experimental validation using a Hardware-in-the-Loop setup, in which the building is emulated while the heat pump, thermal storage, and hydraulic circuits are physically implemented. The results demonstrate the accuracy and effectiveness of the MPC, with indoor temperature deviations remaining low (maximum 2.33 °C·h below and 4.40 °C·h above the set-point) and feasible solutions achieved in 98.52% of the test duration.

1 Introduction

The management of electrified thermal loads in buildings represents a significant opportunity to enhance energy flexibility and thereby supports the transition toward more sustainable energy systems [1]. Energy flexibility refers to the ability of a building to adjust its demand or generation in response to external signals or grid requirements without significantly affecting user comfort [2]. This capability is particularly critical in the context of high penetration of non-dispatchable renewable energy sources, which require energy systems

* Corresponding author: alice.mugnini@uniecampus.it

capable of adapting rapidly to fluctuations in generation. In this regard, buildings can play a fundamental role, as they contribute substantially to total energy demand [3] and offer several opportunities to provide flexibility reserves. Among these, thermal inertia enables a temporary decoupling between demand and generation [4] [5], while the electrification of heating loads through Heat Pumps (HPs) allows additional flexibility to be extracted from thermal demand [6]. However, harnessing this flexibility requires advanced control techniques capable of effectively coordinating HP operation and the available thermal storage. Among these, Model Predictive Control (MPC) is one of the most promising approaches for building heating and cooling systems, due to its ability to combine numerical optimization with real-time feedback [7].

Many studies have demonstrated the ability of MPC to manage building heating demand flexibly and efficiently [8] [9]. For instance, Strauch et al., 2024 [10] applied MPC to a residential building in Karlsruhe, Germany, equipped with a photovoltaic system, battery, HP, electric water heater, and electric vehicle. Their simulations over five winter days show that peak electrical power during the peak periods can be reduced by up to 100% through real-time pricing, demand limiting, load shedding and shifting, and power tracking, while the MPC successfully tracks reference power profiles for 70% of the time, demonstrating its potential to enable thermal demand flexibility without increasing energy costs. Similarly, Klingebiel et al., 2025 [11] developed a data-driven MPC for air-source HPs, demonstrating a 10% improvement in seasonal energy performance compared to a reference controller, thereby confirming the effectiveness of MPC in optimizing energy use. In a larger-scale application, Zanetti et al., 2025 [12] implemented MPC in a large office building heating, ventilation, and air conditioning system in Berkeley, California, integrating dynamic electricity price profiles to shift building demand. Field tests across four seasons indicate peak demand reductions of 40–65% and up to 61% annual cost savings relative to conventional rule-based control, further illustrating how MPC can leverage building thermal mass to provide significant demand flexibility.

These examples represent only a small selection of the many studies demonstrating the effectiveness and potential of MPC for building heating and cooling systems, especially for HP control. However, as noted by Zong et al., 2019 [13], large-scale deployment is limited by the need for dedicated control models, specific infrastructure, and effective management of user interaction and acceptance.

Given the context described above, the aim of this study is to contribute to facilitating the widespread adoption of MPC for residential HPs. To address this challenge, the authors previously developed MPC archetypes for residential buildings with various heating systems, which were experimentally validated [14]. Specifically, three archetypes were developed, differing in the type of heating system: (i) HP with low-temperature radiators ("Archetype 1"), (ii) HP with low-temperature radiators and a hot water tank used as a sensible Thermal Energy Storage (TES) ("Archetype 2"), and (iii) HP with an underfloor heating system ("Archetype 3"). All three archetypes are publicly available in an open GitHub repository [14] [15]. Building on previous work, this study introduces a new archetype configuration, distinct from the existing ones (new "Archetype 4"), which combines an external TES unit with underfloor heating, resulting in a system architecture not previously available [14] [15]. Like the three previously published archetypes, this configuration has been experimentally validated and is publicly available in the same GitHub repository. The validation was conducted using a Hardware-in-the-Loop (HIL) setup, in which the building is emulated while the HP, TES unit, and hydraulic circuits are physically implemented. The MPC is configured to minimize an objective function based on a user-selected penalty signal, which may correspond to electricity price, primary energy consumption, or other operational criteria.

This paper presents the new archetype, describes its features, and reports the results of the experimental tests.

2 Methodology

This section presents the methodology for defining the new MPC archetype. The proposed archetypes integrate control software, and the modelling techniques follow those previously introduced by Mugnini et al. [14]. Here, the main modelling principles are revisited to detail the new archetype, referred to as Archetype 4: a HP with an underfloor heating system and a hot water tank used as TES (Figure 1), following the three archetypes previously developed [14] [15]. An MPC consists of two main components [8] [9]: (i) a predictive model and (ii) an optimizer. The predictive model was implemented using a grey-box approach, ensuring ease of implementation and replicability. The model can be trained with measured data to adapt to real application requirements with minimal programming effort. Section 2.1 describes the predictive model, from the building to the heat pump and TES, while Section 2.2 details the optimizer.

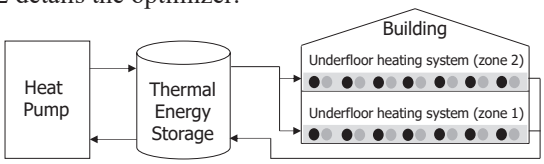

Fig. 1. Schematic diagram of the plant configuration of the new Archetype 4.

2.1 Prediction models

The predictive model for Archetype 4 is composed of four main components: the space heating demand of the building, the heating units, the TES, and the performance of the heat pump. The space heating demand of the building is modelled using the Lumped Parameter Model (LPM) approach, consistent with the method employed for Archetype 3 [14] [15]. The thermal dynamics of the building are represented using a dual-zone configuration, implemented as a 6C10R resistive–capacitive (RC) network. This network includes thermal resistances (R_1–R_{10}), heat capacities (C_1–C_6), and key temperature states: outdoor air, envelope nodes (T_1, T_4), indoor thermal mass (T_3, T_6), and zone air temperatures (T_2, T_5). A schematic of LPM is presented in Figure 2.

All model parameters are determined through a grey-box estimation procedure, calibrated using experimental data collected from the real system. This ensures that the predictive model accurately represents the thermal behavior of the building while remaining adaptable to other similar systems with minimal adjustments.

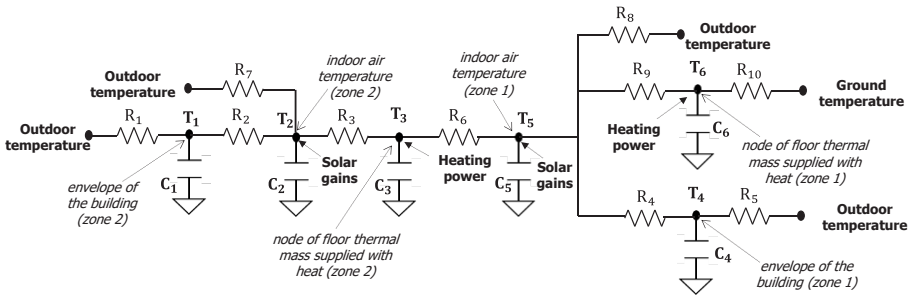

Fig. 2. LPM for building with underfloor heating [14] [15].

Regarding the heating units in MPC Archetype 4, as for Archetype 3 [14] [15], the heating power drawn from the TES (Figure 1) is distributed to the massive nodes of the two thermal zones (Figure 2, nodes 3 and 6). The MPC evaluates the power supplied to each zone by

minimizing the objective function while keeping internal temperatures within the prescribed comfort limits.

The TES is represented by a one-dimensional stratified model [16], divided into four horizontal isothermal layers. Its thermal behavior is captured using the calibrated LPM, with four temperature states (T_h, T_{hm}, T_{cm}, T_c) describing the system.

Key parameters include the layer capacities, equally distributed from the total tank capacity, the heat loss coefficient, and the conductive heat transfer to the surrounding environment (Figure 3). This TES model differs from that used in [14], where ten thermal nodes were employed. Its performance has been investigated in a previous study by the authors [17] in the context of the radiator-based archetype (Archetype 2 in Mugnini et al. [14]). In that study, the authors demonstrated that this model configuration (a *one-dimensional* model according to Raccanello et al., [16]) is able to better exploit the thermal inertia of the storage, showing larger temperature fluctuations and lower errors in predicting the temperatures of the thermal layers in the TES.

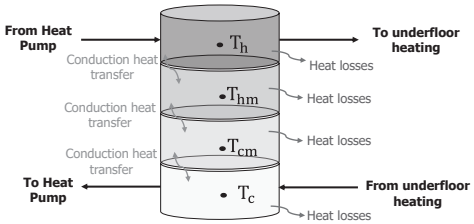

Fig. 3. LPM for TES [17].

Finally, the HP performance model describes heating capacity (HC) and electrical power consumption (Pl) as functions of condenser and evaporator temperatures and the modulation level, expressed by the Capacity Ratio (CR), i.e., the ratio of required to nominal thermal power. Both HC and Pl are represented using polynomial equations, with a penalty factor applied to Pl to account for performance degradation when CR falls below the minimum modulation. Polynomial coefficients are derived from manufacturer technical catalogues. A complete description, including all equations and calibration details, is provided in Mugnini et al. [14].

2.2 Optimizer

In this subsection, the optimization framework implemented in the MPC archetypes is presented. As with the first three archetypes discussed in Mugnini et al. [14], a full description of Archetype 4 is provided in Annex A.

Figure 4 depicts a typical configuration of an MPC applied to the control of a HP heating system. The MPC is composed of two main elements: a predictive model and an optimizer.

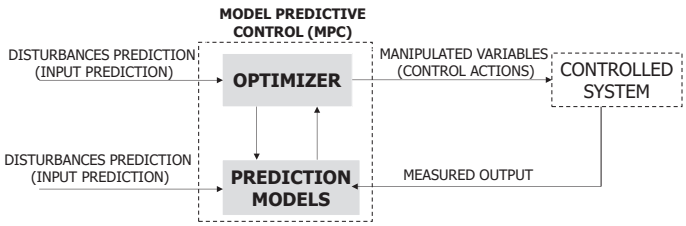

Fig. 4. Overview diagram of the MPC structure.

The predictive model is responsible for estimating the energy demand of the building over a specified time period, known as the prediction horizon, based on the influence of uncontrolled factors, or disturbances. In the archetypes, disturbances include weather-related variables such as outdoor air temperature, ground temperature, and global horizontal solar irradiation. These inputs must be forecasted over the prediction horizon, and at each control interval, the corresponding time series of the disturbance variables should be available according to the control timestep.

Based on the predicted building response, the optimizer calculates the control actions that minimize a chosen objective function while respecting system constraints. In the MPC archetypes presented here, the default objective is to minimize electrical power consumption over the prediction horizon. The control code allows this objective to be adjusted via a user-defined penalty signal, which can also be configured to account for other factors, such as electricity price, if desired. Constraints in the optimization include maintaining thermal comfort in the building zones, expressed as limits on indoor air temperatures, as well as operational limits on the heating system, including flow rates and supply temperatures. Following the "*receding horizon*" approach, only the first control action of the prediction horizon is applied. The horizon is then shifted forward, and the optimization is repeated at the next timestep. The control actions determined by the MPC include switching the HP on or off, setting the condenser water supply temperature, switching on or off the heat supply to the thermal zones, and evaluating the optimizer solution status to determine whether the backup RBC (Ruled-Based Control) should be activated in case of an infeasible solution. The RBC is a standard thermostat keeping indoor temperature within the comfort range.

The optimization problem is solved using the Gekko package in Python [18], and if the MPC fails to identify a feasible solution, a backup control strategy, implemented as a rule-based on/off controller, is employed to ensure occupant comfort [14].

3 Experimental setup for MPC archetype validation

As with the other three validated archetypes [14], Archetype 4 was validated through an experimental campaign. The setup uses a real water-to-water HP to meet the space-heating demand of a representative Belgian residential building [19]. In the HIL configuration, the HP [20] and the TES [21] operate as physical components, while the building is emulated in Modelica. The main features of the HIL setup are summarized in Table I.

Table 1. Key features of the HIL setup.

Characteristics of the HP, TES and building	Value
B0/W35 (condenser/electrical power) [21]	7.98 kW / 1.79 kW
Volume of the TES	750 liters
Thermal transmittance of the building (walls / windows)	0.24 W m-2K-1 / 1.45 W m-2K-1
Net floor area of the building (2 floors / thermal zones)	194 m²
Nominal heat loss of the building at –8 °C	9.4 kW

The heat source and building load are emulated via heat exchangers with adjustable setpoints controlled by 3-way valves, and a 750-liter TES with monitored thermal stratification is integrated into the loop. TES temperatures were recorded at four heights along the tank, while the source and sink conditions were imposed through controlled supply-temperature setpoints.

The MPC framework runs through two Python scripts communicating via a local database: one governs the HIL with a 15-s timestep, and the other executes the MPC optimization every 10 minutes. A Modelica building model is imported into Python via FMPy [22] with Python acting as the master controller for real-time synchronization. The HP communicates through a Modbus interface, providing remote access to temperatures, flow rates, and other operating data. Experimental data were logged at 15-second intervals. Figure 5 shows the arrangement of communication between the simulation and the experiment.

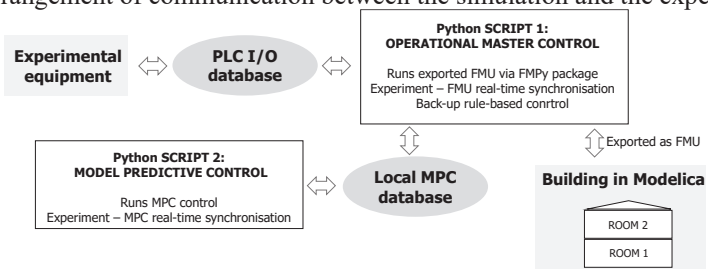

Fig. 5. Setup of communication links in the HIL experiment.

4 Prediction models training and validation

As described in subsection 2.1, LPMs are employed to predict both space heating demand and TES dynamics within the MPC framework. For validation purposes, a detailed Modelica-based emulator reproduces the behaviour of the building and heating system in the laboratory. The grey-box models are trained using a combination of emulator simulations and experimental heat pump measurements. Further details can be found in [14]. The dataset covers three winter months (December to February) from a Typical Meteorological Year for Belgium (Uccle), with a 10-minute timestep. A 25-day period (starting January 6, day 37) was selected for training as it best represents the range of outdoor temperatures in the full dataset. Model performance was then evaluated on validation periods before and after this training interval. Further details can be found in [14], which also describes the building model corresponding to Archetype 3 used in this study.

For the TES, measured data refer to 100-hour charge/discharge cycles, as described in [21]. The training period covers hours 24 to 72, while validation was performed on hours 0–24 (period 1) and 72–100 (period 2). This segmentation produced the most accurate model predictions. Further details, including the training results reported here, can be found in [17].

Table II summarizes the main validation results, reporting the RMSE (Root Mean Square Error) of thermal node temperatures for both training and validation periods, with the node notation corresponding to the symbols shown in Figures 2 and 3. During the training period, RMSE values for all thermal nodes remain below 0.7 °C, while in the validation periods they mostly stay under 1.2 °C, confirming the predictive accuracy of the LPMs.

Table 2. Training and validation results for LPMs models in archetype 4 (RMSE in °C) [14] [15].

Thermal node	Training	Validation period 1	Validation period 2
T_1	0.67	0.71	1.20
T_2	0.32	0.36	0.55
T_3	0.39	0.40	0.66
T_4	0.67	0.70	1.19

T_5	0.31	0.37	0.51
T_6	0.47	0.49	0.70
T_h	0.58	0.53	0.50
T_{hm}	0.36	0.37	0.37
T_{cm}	0.31	0.31	0.34
T_c	0.58	0.68	0.79

5 Results

This section presents the results of the new MPC Archetype 4 based on an 8-day experiment, using the representative period method of [19]. The MPC operated with a 10-minute timestep and a 24-hour prediction horizon.

Figure 6 shows the comparison between the indoor air temperatures in the two thermal zones of the building, thermal zone 1 (6a) on the ground floor and thermal zone 2 (6b) on the first floor, as predicted by the MPC model and as measured during the validation test. Although the prediction model slightly overestimates the temperatures in both thermal zones, the MPC is effective in maintaining the imposed setpoint throughout the experimental campaign. The RMSE between measured and predicted indoor air temperatures is 0.71 °C for T_5 in thermal zone 1 and 0.60 °C for T_2 in thermal zone 2. Predictions for the other thermal nodes are also satisfactory, with values of 0.84 °C (T_4) and 0.89 °C (T_6) in zone 1, and 0.85 °C (T_1) and 1.37 °C (T_3) in zone 2. The symbols used for the thermal nodes are those reported in Figure 2.

Overall, the MPC effectively maintains occupant comfort, as reflected by the low degree-hours of discomfort in both thermal zones. In zone 1, the indoor temperature remained below the setpoint for 2.33 °C·h and above it for 4.40 °C·h, while in zone 2 the corresponding values were 0.73 °C·h and 1.31 °C·h. These results indicate that the indoor environment is generally kept close to the desired setpoints throughout the experiment.

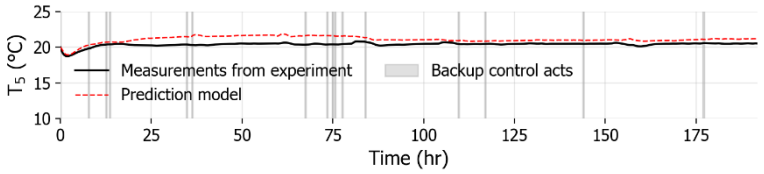

(a)

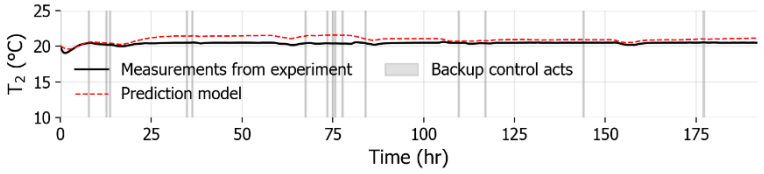

(b)

Fig. 6. Experimental validation results for MPC archetype 4, comparing the internal air temperatures measured in the building with the predictions from the model: (a) thermal zone 1 (T_5 in Figure 2) and (b) thermal zone 2 (T_2) in Figure 2

The prediction of the TES model is illustrated in Figure 7, which compares the temperatures predicted by the MPC model with the measured values at the highest thermal node (7a) and the lowest thermal node (7b). The symbols used for the thermal nodes are those reported in Figure 3. The RMSE values are 0.76 °C for T_h, 2.86 °C for T_c, 0.52 °C for T_{hm}, and 0.49 °C for T_{cm}. Overall, the relatively low RMSE indicates that the TES model accurately captures the thermal storage dynamics, showing good agreement between predictions and measurements.

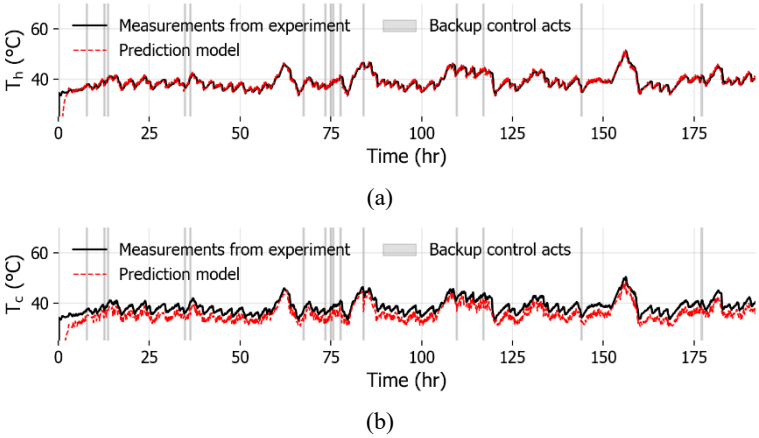

Fig. 7. Experimental validation results for MPC Archetype 4, showing the comparison between measured TES temperatures and model predictions: (a) upper layer (T_h in Figure 3) and (b) lower layer (T_c in Figure 3).

To conclude, the results confirm the strong effectiveness of the optimization process within the MPC. Consistent with the findings reported for the other archetypes in Mugnini et al., 2024, the optimizer reliably identified feasible solutions, achieving a success rate of 98.52% for Archetype 4. The backup controller (i.e., the RBC) intervened for only 2.83 hours, as highlighted by the grey areas in Figures 6 and 7, further demonstrating the robustness and reliability of the proposed control strategy.

6 Conclusions

This study presented a novel Model Predictive Control (MPC) approach specifically developed for Heat Pump systems with underfloor heating and an external thermal energy storage unit. The proposed control strategy extends previous MPC archetypes aimed at simplifying the design of predictive controllers while enabling large-scale implementation in building heating systems. The experimental validation, conducted through a Hardware-in-the-Loop setup over an eight-day period, demonstrated the practical effectiveness and accuracy of the proposed control approach. Results indicate that the controller successfully maintains indoor air temperatures close to the desired setpoints, with Root Mean Square Errors of 0.71°C and 0.60 °C for the main thermal nodes of the ground and first floor, respectively. Comfort was consistently preserved, with temperature deviations remaining within 2.33 °C h below and 4.40 °C h above the setpoint. The Thermal Energy Storage model also showed good agreement between predicted and measured values, with Root Mean Square Errors of 0.76 °C for the upper layer. The optimization process within the control strategy proved highly reliable, achieving feasible solutions in 98.52 % of the time, while the backup rule-based controller intervened for only 2.83 hours over the entire experiment. These findings confirm the robustness, accuracy, and practical applicability of the proposed control

approach, demonstrating its potential to ensure occupant comfort and efficient operation in complex building heating systems.

The MPC Archetype 4 presented in this study is available in a public GitHub repository: github.com/diismunivpm/PredictiveArchHP

References

1. European Commission. (2019) The European Green Deal.
2. Jensen S.Ø., Marszal-Pomianowska A., Lollini R., Pasut W., Knotzer A., Engelmann P., Stafford A., Reynders G. (2017) IEA EBC Annex 67 Energy Flexible Buildings. Energy and Buildings, 155, 25–34. https://doi.org/10.1016/j.enbuild.2017.08.044
3. European Commission. (2023) Energy Performance of Buildings Directive.
4. Lind J., Möllerström E., Averfalk H., Ottermo F. (2023) Energy flexibility using the thermal mass of residential buildings. Energy and Buildings, 301, 113698. https://doi.org/10.1016/j.enbuild.2023.113698
5. Tunçbilek E., Yıldız Ç., Arıcı M., Ma Z., Awan M.B. (2023) Thermal energy storage for enhanced building energy flexibility. In: Ma Z., Arıcı M., Shahsavar A. (Eds.), Building Energy Flexibility and Demand Management. Academic Press, 89–119. https://doi.org/10.1016/B978-0-323-99588-7.00004-3
6. Abd Alla S., Bianco V., Scarpa F., Tagliafico L.A. (2022) Electrification of the residential heat demand: An analysis of the power market potential to accommodate heat pumps. Thermal Science and Engineering Progress, 27, 101173. https://doi.org/10.1016/j.tsep.2021.101173
7. Drgoňa J., Arroyo J., Cupeiro Figueroa I., Blum D., Arendt K., Kim D., Perarnau Ollé E., Oravec J., Wetter M., Vrabie D.L., Helsen L. (2020) All you need to know about model predictive control for buildings. Annual Reviews in Control, 50, 190–232. https://doi.org/10.1016/j.arcontrol.2020.09.001
8. Saloux E., Candanedo J.A., Vallianos C., Morovat N., Zhang K. (2025) From theory to practice: A critical review of model predictive control field implementations in the built environment. Applied Energy, 393, 126091. https://doi.org/10.1016/j.apenergy.2025.126091
9. Serale G., Fiorentini M., Capozzoli A., Bernardini D., Bemporad A. (2018) Model Predictive Control (MPC) for Enhancing Building and HVAC System Energy Efficiency: Problem Formulation, Applications and Opportunities. Energies, 11, 631. https://doi.org/10.3390/en11030631
10. Strauch P., Wang W., Langner F. (2024) Model predictive control for demand flexibility of a residential building with multiple distributed energy resources. Energy and Buildings, 305, 113884. https://doi.org/10.1016/j.enbuild.2023.113884
11. Klingebiel J., Beckschulte M., Will F., Vering C., Müller D. (2025) Multi-objective model predictive control for air-source heat pumps: Leveraging system flexibility to simultaneously reduce noise and increase efficiency. Applied Thermal Engineering, 278, 126926. https://doi.org/10.1016/j.applthermaleng.2025.126926
12. Zanetti E., Blum D., Fu H., Weyandt C., Pritoni M., Piette M.A. (2025) Commercial building HVAC demand flexibility with model predictive control: Field demonstration and literature insights. Energy and Buildings, 345, 116097. https://doi.org/10.1016/j.enbuild.2025.116097

13. Zong Y., Su W., Wang J., Rodek J.K., Jiang C., Christensen M.H., You S., Zhou Y., Mu S. (2019) Model Predictive Control for Smart Buildings to Provide the Demand Side Flexibility in the Multi-Carrier Energy Context: Current Status, Pros and Cons, Feasibility and Barriers. Energy Procedia, 158, 3026–3031. https://doi.org/10.1016/j.egypro.2019.01.981
14. Mugnini A., Evens M., Arteconi A. (2024) Model predictive controls for residential buildings with heat pumps: Experimentally validated archetypes to simplify the large-scale application. Energy and Buildings, 320, 114632. https://doi.org/10.1016/j.enbuild.2024.114632
15. GitHub repository for MPC archetypes. (2024) https://github.com/diismunivpm/PredictiveArchHP
16. Raccanello J., Rech S., Lazzaretto A. (2019) Simplified dynamic modeling of single-tank thermal energy storage systems. Energy, 182, 1154–1172. https://doi.org/10.1016/j.energy.2019.06.088
17. Mugnini A., Evens M., Felicetti R., Ferracuti F., Arteconi A. (2025) Experimental analysis on the role of modeling sensible Thermal Energy Storages in Model Predictive Controls applied to buildings with Heat Pumps. REHVA HVAC World Congress CLIMA 2025.
18. Beal L.D.R., Hill D.C., Martin R.A., Hedengren J.D. (2018) GEKKO Optimization Suite. Processes, 6, 106. https://doi.org/10.3390/pr6080106
19. Evens M., Arteconi A. (2023) Representative cycle for heat pump energy flexibility evaluations – A comparative simulation study of existing day selection procedures to a new consecutive day procedure. Energy and Buildings, 297, 113443. https://doi.org/10.1016/j.enbuild.2023.113443
20. Daikin. (2020) Geothermal HP EGSAX06D9W.
21. Evens M., Arteconi A. (2024) Design energy flexibility within a comfort and climate box – An experimental evaluation of the internal heat pump control effects. Applied Thermal Engineering, 254, 123842. https://doi.org/10.1016/j.applthermaleng.2024.123842
22. Viessmann. (2019) Vitocell 100-E Technical Specifications.

ANNEX A: detailed model of new MPC archetype 4

Archetype 4 refers to a residential building equipped with a HP, an underfloor heating system, and a hot water tank used as TES. The configuration with two thermal zones is described. The equations of the RC-network model are presented below, together with the definition of the symbols as reported in Figure 2 of the paper.

$$C_1\dot{T}_1 = (T_{out} - T_1)/R_1 + (T_2 - T_1)/R_2 \quad \text{A-1}$$

$$C_2\dot{T}_2 = (T_{out} - T_2)/R_7 + (T_1 - T_2)/R_2 + (T_3 - T_2)/R_3 + f_2\dot{G} \quad \text{A-2}$$

$$C_3\dot{T}_3 = (T_2 - T_3)/R_3 + (T_5 - T_3)/R_6 + \dot{Q}_2 \quad \text{A-3}$$

$$C_4\dot{T}_4 = (T_5 - T_4)/R_4 + (T_{out} - T_4)/R_5 \quad \text{A-4}$$

$$C_5\dot{T}_5 = (T_{out} - T_5)/R_8 + (T_3 - T_5)/R_6 + (T_6 - T_5)/R_9 + (T_4 - T_5)/R_4 + f_1\dot{G} \quad \text{A-5}$$

$$C_6\dot{T}_6 = (T_{grd} - T_6)/R_{10} + (T_5 - T_6)/R_9 + \dot{Q}_1 \quad \text{A-6}$$

Where T_1, T_2, T_3, T_4, T_5,and T_6denote the temperatures of the thermal nodes defined in Figure 2, and C_1, C_2, C_3, C_4, C_5,and $C_6$are the corresponding thermal capacities. Specifically, $(T_1, C_1)$and (T_4, C_4)represent the temperatures and thermal masses of the building envelope of Thermal Zone 2 (second floor) and Thermal Zone 1 (first floor), respectively, each exchanging heat with the outdoor temperature T_{out} through the resistances $R_1$and R_{10}. The indoor air temperatures and capacities of the two thermal zones are given by $(T_2, C_2)$and (T_5, C_5), interacting with the outdoor environment through $R_7$and R_8, with the envelope nodes through R_2, R_3, R_9, and with the internal masses via R_4. The nodes $(T_3, C_3)$and (T_6, C_6)correspond to the building's thermal masses in Zones 2 and 1, receiving the thermal inputs $\dot{Q}_2$and $\dot{Q}_1$, and exchanging heat with adjacent nodes through R_3, R_4, and R_6. Solar gains are represented by $f_1\dot{G}$and $f_2\dot{G}$, where $f_1$and $f_2$are the identified solar gain factors and $\dot{G}$is the global horizontal irradiation. The ground temperature T_{grd}, assumed equal to 13°C, exchanges heat with node T_4via R_5.

The hot water tank model, consisting of four layers, is described by the following equations, with reference to Figure 3 of the paper:

$$C_{tes}\dot{T}_h = \dot{m}_{cond}c_p(T_{out_{cond}} - T_h) + (\dot{m}_{ff} + \dot{m}_{sf})c_p(T_{hm} - T_h) + k(T_{hm} - T_h) + L(T_h - T_{env}) \quad \text{A-7}$$

$$C_{tes}\dot{T}_{hm} = \dot{m}_{cond}c_p(T_h - T_{hm}) + (\dot{m}_{ff} + \dot{m}_{sf})c_p(T_{cm} - T_{hm}) + k(T_{cm} - T_{hm}) + k(T_h - T_{hm}) + L(T_{hm} - T_{env}) \quad \text{A-8}$$

$$C_{tes}\dot{T}_{cm} = \dot{m}_{cond}c_p(T_{hm} - T_{cm}) + (\dot{m}_{ff} + \dot{m}_{sf})c_p(T_c - T_{cm}) + k(T_c - T_{cm}) + k(T_{hm} - T_{cm}) + L(T_{cm} - T_{env}) \quad \text{A-9}$$

$$C_{tes}\dot{T}_c = \dot{m}_{cond}c_p(T_{cm} - T_c) + \dot{m}_{ff}c_p(T_{out_{ff}} - T_c) + \dot{m}_{sf}c_p(T_{out_{sf}} - T_c) + k(T_{cm} - T_c) + L(T_c - T_{env}) \quad \text{A-10}$$

Where T_h, T_{hm}, T_{cm},and $T_c$denote the temperatures of the four layers of the hot water tank (Figure 3), and $C_{tes}$is the thermal capacity of each layer. The top (T_h) and bottom (T_c) layers exchange heat with the condenser output $T_{out,cond}$and the returning floor heating water $T_{out,ff}$and $T_{out,sf}$, respectively. The intermediate layers (T_{hm}, T_{cm}) interact with adjacent layers via conduction $k(T_{adjacent} - T)$and with the heating circuits through $\dot{m}_{ff}$and $\dot{m}_{sf}$. All the layers experience environmental losses $L(T - T_{env})$, with the ambient temperature T_{env}assumed equal to 10 °C. In this grey-box modeling approach, C_{tes}, k, and L are identified as key model parameters, while $\dot{m}_{cond}$, $\dot{m}_{ff}$, and $\dot{m}_{sf}$represent the known mass flows.

The objective of the MPC is to minimize the primary energy consumption, namely the electricity drawn from the grid, while keeping the air temperature in both thermal zones

within the range set by the thermostat. This allows the control strategy to exploit the flexibility provided by the thermostatically controlled loads. For Archetype 4 the temperature bounds are 19.5°C to 20.5°C.

The MPC in Archetype 4 manipulates the HP modulation for thermal zones 1 and 2 (CR_1 and CR_2), as well as the water flow and temperatures at the condenser ($\dot{m}_{cond}$, $T_{in,cond}$, $T_{out,cond}$). Control actions include the on-off signal for the HP ($CTRL_{HP}$), setpoints for the condenser temperature ($COND_{SET}$), on-off signals for the heat service to zones 1 and 2 ($CTRL_{SH1}$, $CTRL_{SH2}$), and an optimizer solution status, used to evaluate if the backup RBC should be activated ($CTRL_{OPT}$). The measured outputs comprise the temperatures of the thermal nodes of the building (T1–T6 according to Figure 2 in the paper), thermal powers supplied to the zones ($\dot{Q}_{h1}, \dot{Q}_{h2}$), the condenser outlet temperature ($T_{out,cond}$), the evaporator inlet temperature ($T_{in,evap}$), and the TES layer nodes, namely top (T_h), bottom (T_c), upper-middle (T_{hm}), and lower-middle (T_{cm}) temperatures (according to Figure 3 in the paper).

The MPC applies the receding horizon control logic, according to which only the first value computed for the control actions is applied, and the prediction horizon of 24 hours always moves forward by one time step of 10 minutes. A time step of 10 minutes is used consistently, according to the data provided for the case study.

Below is the extensive writing of the optimization problem in the MPC archetype 4.

Objective function:

$$minimize\left(\sum_{t=0}^{PH} p(t)P_l(T_{out_{cond}}(t), T_{in_{evap}}(0), CR_1(t) + CR_2(t))\right) \quad \text{A-11}$$

where $p(t)$is a user-defined penalty function, for example representing the electricity price (in this study it is always set to one, corresponding to minimizing the total electrical energy consumption). $P_l$denotes the electrical power of the heat pump, and PH is the prediction horizon. The value measured at t equal to 0 hour is kept constant throughout the PH ($T_{in_{evap}}(0)$).

Limits for decision variables:

$$\forall\, t\ in\ PH \quad 0 \le CR_1(t) \le 1 \quad \text{A-12}$$

$$\forall\, t\ in\ PH \quad 0 \le CR_2(t) \le 1 \quad \text{A-13}$$

$$\forall\, t\ in\ PH \quad 25\ °C \le T_{out_{cond}}(t) \le 55\ °C \quad \text{A-14}$$

$$\forall\, t\ in\ PH \quad 0\ kg\ s^{-1} \le \dot{m}_{cond}(t) \le 0.256\ kg\ s^{-1} \quad \text{A-15}$$

$\dot{m}_{ff}$ and $\dot{m}_{sf}$ are calculated as intermediate variables from design flows and TES top/bottom temperatures, not directly controlled.

Constraints:

$$\forall\, t\ in\ PH \quad 19.5°C \le T_{z_1}(t) \le 20.5°C \quad \text{A-16}$$

$$\forall\, t\ in\ PH \quad 19.5°C \le T_{z_2}(t) \le 20.5°C \quad \text{A-17}$$

$$\forall\, t\ in\ PH \quad 30°C \le T_h(t) \le 50°C \quad \text{A-18}$$

$$\forall\, t\ in\ PH \quad CR_1(t) + CR_2(t) \le 1 \quad \text{A-19}$$

$$\forall\, t\ in\ PH \quad T_h(t) > T_c(t) \quad \text{A-20}$$

$$\forall\, t\ in\ PH \quad T_{out_{cond}}(t) - T_c(0) \ge \Delta T_{design} \quad \text{A-21}$$

With ΔT_{design} is equal to 3 °C and c_p equal to 4190 J kg^{-1} K^{-1}, where ΔT_{design} represents the considered design temperature difference in the storage tank.

Control actions:

$$CTRL_{HP} = CR_1(0) + CR_2(0) \quad \text{A-22}$$

$$COND_{SET} = T_{out\,cond}(0) \quad \text{A-23}$$

$$CTRL_{SH_1} = 1\ if\ CR_1(0) > 0, 0\ otherwise \quad \text{A-24}$$

$$CTRL_{SH_2} = 1\ if\ CR_2(0) > 0, 0\ otherwise \quad \text{A-25}$$

$$\forall\ t\ in\ PH \quad T_h(t) > T_c(t) \quad \text{A-26}$$

$$CTRL_{OPT} = 1\ if\ a\ feasible\ solution\ is\ found, 0\ otherwise \quad \text{A-27}$$

When $CTRL_{OPT}$ is equal to 0, a rule-based backup control is activated, which is a simple thermostat that maintains the setpoint within the same ranges.

Finally, Figure A-1 shows an operational diagram of how the MPC of Archetype 4 is applied to the system to be controlled.

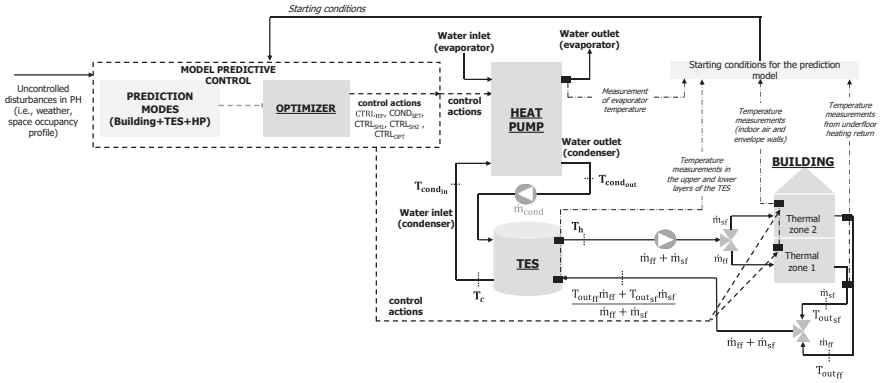

Fig. **A-1**. Operational schematic of the Archetype 4 MPC applied to the controlled system.